

# The shell model approach to the rotating turbulence

M. Reshetnyak<sup>a,b,\*</sup>, B. Steffen<sup>c</sup>

*Institute of the Physics of the Earth, Russian Acad. Sci, 123995 Moscow, Russia<sup>a</sup>*

*Research Computing Center of Moscow State University,  
119899, Moscow, Russia<sup>b</sup>*

*Central Institute for Applied Mathematics (ZAM)  
of Forshungszentrum Jülich, Germany<sup>c</sup>*

---

## Abstract

Applications of the shell model of turbulence to the case of rapidly rotating bodies are considered. Starting from the classical GOY model we introduce the Coriolis force and obtain a  $\sim k^{-2}$  spectrum for 3D hydrodynamical turbulence for the free decay regime as well for the regime with external forcing. Additional modifications of the GOY model providing a realistic form of the helicity are proposed.

*Key words:* Shell model, Kolmogorov's spectrum, force balance,  $\alpha$ -effect

---

## 1 Introduction

The influence of rotation on the properties of the hydrodynamical turbulence is of the great importance. This problem appears in the various geophysical and astrophysical applications [1] and it requires special treatment. So far the direct 3D numerical simulations, where implementation of the Coriolis force is trivial, cannot provide a long enough inertial range of spectrum to reveal its scaling laws [2], thus different approaches are needed.

Though the possibility of transition from 3D-turbulence state to the two-dimensional turbulence due to rotation was already predicted by Batchelor

---

\* Corresponding author.

E-mail address: maxim@uipe-ras.scgis.ru (M. Reshetnyak).

many years ago [3], only now is the qualitative description of this processes developing [4], [5]. Having in mind the similar situation in the MHD turbulence [6], where the magnetic field plays the same role as the rotation in reducing the dimension of the problem, the authors proposed that the Coriolis force introduces a new characteristic time. This time should be used instead of the characteristic turn-over time based on the Kolmogorov's estimate. Then, instead of Kolmogorov's  $-5/3$  slope the spectrum will have a  $-2$  slope. It appears that this approach is in agreement with the direct numerical calculations [7] and the experiments [8]. The formal simplicity of this phenomenological approach attracts us to implement it in the more complicated models of turbulence and to check the results for self-consistence. For this aim we use the well-known homogeneous isotropical GOY shell model (see overview in [9]) and modify it to the case of rotation. The proposed model is tested for the regimes of the free-decay turbulence and for the regime with external forcing. We also consider a situation where a non-zero average helicity is generated. This regime finds its application in the mean-field dynamo problems.

## 2 Basic equations

The evolution of conductive incompressible liquid ( $\nabla \cdot \mathbf{V} = 0$ ), rotating with the angular velocity  $\Omega$ , can be described by the Navier-Stokes equation:

$$R_o \left( \frac{\partial \mathbf{V}}{\partial t} + (\mathbf{V} \cdot \nabla) \mathbf{V} \right) = -\nabla P + \mathbf{F} + E \nabla^2 \mathbf{V}. \quad (1)$$

Eq.(1) is scaled with the large scale of the body  $L$ ; velocity  $V$ , pressure  $P$  and time  $t$  are measured in  $\eta/L$ ,  $\rho\eta^2/L^2$  and  $L^2/\eta$ , where  $\eta$  is a magnetic diffusion,  $\rho$  is density,  $R_o = \eta/2\Omega L^2$  and  $E = \nu/2\Omega L^2$  are the Rossby and Ekman numbers, respectively and  $\nu$  is the kinematic viscosity. (This kind of scaling takes its origin in geodyamo problems [10].) The force  $\mathbf{F} = \mathbf{F}_c + \mathbf{f}$  includes the Coriolis effect:

$$\mathbf{F}_c = -\mathbf{1}_z \times \mathbf{V} \quad (2)$$

and a prescribed part  $\mathbf{f}$ . Here  $\mathbf{1}_z$  is the unit vector along the axis of rotation.

It is worth to note that, in the limit of the vanishing viscosity and absence of the external force ( $\mathbf{f} = 0$ ), equation (1) conserves kinetic energy  $E_k = V^2/2$ . For the two-dimensional flow the other integral of motion is the enstrophy  $E_\Omega = (\nabla \times \mathbf{V})^2$  and for 3D case the hydrodynamical helicity  $H = \mathbf{V} \cdot (\nabla \times \mathbf{V})$  is conserved (see for details, e.g., [9; 1]).

### 3 Shell model equations

The idea of the shell model approach is to mimic the original equation (1) by a dynamical system with  $n_{max}$  complex variables  $u_1, u_2, \dots, u_{n_{max}}$  which represent the typical magnitude of the velocity on a certain length scale. The Fourier space is divided into  $n_{max}$  shells and each shell  $k_n$  consists of a set of wave vectors  $\mathbf{k}$  such that  $k_0 2^n < |\mathbf{k}| < k_0 2^{n+1}$ , and thus each shell corresponds to an octave of the wave numbers. Variable  $u_n$  is the velocity difference over length  $\sim 1/k_n$ , so that there is one degree of freedom per shell. The coupling between shells is considered to preserve the main symmetries and properties of equation (1). Of course, the shell model is a simplified form of the description of the turbulence, nevertheless, it is a reasonable tool in the studies of turbulence. Here and after we will refer to the GOY model [9], which has the form:

$$R_o \frac{du_n}{dt} = R_o i k_n \left( u_{n+1}^* u_{n+2}^* - \frac{\epsilon}{2} u_{n-1}^* u_{n+1}^* - \frac{1-\epsilon}{4} u_{n-2}^* u_{n-1}^* \right) - E k_n^2 u_n + F_n, \quad (3)$$

where  $\epsilon$  is a free parameter,  $*$  is the complex conjugate.

In the inviscid limit ( $E \rightarrow 0$ ) and free forcing ( $F = 0$ ) equation (3) has two integrals. The first integral is the kinetic energy

$$E_k = \sum_n |u_n|^2. \quad (4)$$

The other integral is the so-called generalized enstrophy

$$\widehat{H} = \sum_n [\text{sgn}(\epsilon - 1)]^n k_n^{\alpha(\epsilon)} |u_n|^2, \quad (5)$$

with  $\alpha(\epsilon) = -\log_2(|\epsilon - 1|/2)$ . For  $\epsilon > 1$   $\widehat{H}$  is always positive

$$\widehat{H} = H = \sum_n n k_n^{\alpha(\epsilon)} |u_n|^2. \quad (6)$$

For  $\epsilon = 5/4$  its dimension coincides with dimension of the enstrophy, which is an integral of motion in 2D problem. That is the reason why  $\epsilon = 5/4$  usually is associated with the two-dimensional space. Cases with  $\epsilon < 1$  correspond closer to the helicity integral and can have different sign. In the case of  $\epsilon = 1/2$  the dimension of  $\widehat{H}$  is equal to the dimension of the hydrodynamical helicity, so this case corresponds to 3D space. It is known that the 3D shell model can reproduce Kolmogorov's spectrum  $\sim k^{-5/3}$ . The situation in 2D space ( $\epsilon = 5/4$ ) is more complicated. Application of an external force at some wave

number  $k_f$  gives rise to two spectral regimes: for  $k > k_f$  the direct spectrum for the enstrophy, and the spectrum for the inverse energy cascade with the slope similar to Kolmogorov's  $-5/3$  for  $k < k_f$ . The slope of the inverse cascade spectrum for enstrophy depends on  $\epsilon$  and can change its value from  $-3$  for  $\epsilon = 5/4$  to  $-5/3$  for  $\epsilon \approx 10$  [11]. Here and after we will consider only the direct cascades in the 3D case with  $\epsilon = 1/2$ .

To introduce effect of rotation in the GOY model we propose that the Coriolis force can be written in the form:

$$F_c = -iC_r u, \tag{7}$$

where the constant real coefficient  $C_r$  is introduced for convenience. It is easy to see that the work of the Coriolis force (7) is zero ( $u_n^* F_{cn} + u_n F_{cn}^* = 0$ ) and no additional energy is introduced into the system (3) at any scale. This property of the force (7) coincides with the property of the Coriolis force in 3D space (1).

Having in mind that in derivation of the shell model equations (3) all external potential forces, as well as pressure, were already excluded using condition of incompressibility ( $\nabla \cdot \mathbf{V} = 0$ ),  $F_c$  corresponds to the curl part of the Coriolis force. We will return to this point when the case with the several forces will be considered in section 5.

In the following sections we will consider the applications of the shell model (3, 7) to the free decay turbulence (section 4) and to the regime with the external forcing (section 5). Special attention will be paid to the helicity generation produced in such models (section 6).

## 4 Free decay hydrodynamic turbulence

To analyze behaviour of the hydrodynamical turbulence without forcing we start from the free decay regime ( $f = 0$ ). After some intermediate regime for the case without rotation ( $F_c = 0$ ) the Kolmogorov's spectrum ( $-5/3$ ) recovers, see figures 1, 2. The sharp breaks in the spectra at the large wave numbers correspond to the Kolmogorov's diffusion scale  $k_d$ . The estimate based on the balance of the inertial  $R_o k_n u_n^2$  and diffusion  $E k_n^2 u_n$  terms leads to  $k_d \sim \frac{R_o}{E} u_n$ .

As was predicted in [4], [5], introduction of rotation ( $F_c \neq 0$ ) gives rise to a new time scale  $\tau_d \sim \Omega^{-1}$ . For  $R_o \ll 1$ ,  $\tau_d$  is already shorter than the characteristic time in the Kolmogorov's regime  $\tau_{dn} \sim k_n^{-2/3}$ . A simple dimensional analysis

leads to the estimate of the rate of the energy dissipation

$$\varepsilon \sim \tau(k)k^4 E^2(k), \quad (8)$$

where  $\tau$  is the characteristic time and  $E(k)$  is the spectral energy density. In the case of the Kolmogorov's turbulence  $\tau \sim (k^3 E)^{-1/2}$  and

$$E(k) \sim \varepsilon^{2/3} k^{-5/3}. \quad (9)$$

If the effect of rotation is sufficient, then substitution of  $\tau \sim \Omega^{-1}$  into (8) leads to the rotation spectrum law [5]:

$$E(k) \sim (\Omega \varepsilon)^{1/2} k^{-2}. \quad (10)$$

Starting simulations from the initial field obtained in the non-rotating regime, after a short time period the original Kolmogorov's spectrum splits into two parts with two different slopes, see Fig. 1, 2. The change in the slope ( $n_\Omega \in [10, 19]$  and  $k_n = 2^n$ ) corresponds to  $k_\Omega = \frac{C_\Omega^2}{Ro^{u_{n_\Omega}}}$ , where  $C_\Omega = 1.22 \div 1.87$  [5]. This estimate can be obtained from balancing the inertial term and the Coriolis force. If for the large scales the Coriolis term is larger than the non-linear term, the spectrum decays as  $\sim k^{-2}$ . In this case non-linear term do not depend on  $k$  and the Coriolis term decays as  $\sim k^{-1/2}$ . The further behaviour depends on how long the spectrum is and where the Kolmogorov's wave number  $k_d$  lies. If  $k_\Omega > k_d$ , then the whole spectrum decays as  $\sim k^{-2}$ . In the other case ( $k_\Omega < k_d$ ) the Kolmogorov's spectrum  $-5/3$  for  $k > k_\Omega$  reappears. This situation is demonstrated in the figures 1, 2. As the whole kinetic energy of the system decays in time, the  $k_\Omega$  moves in to the region of the large wave numbers. Note that the situation can be complicated by the high order effects, as the decay rates of the both spectra are different.

## 5 Convection with external forcing

To consider the evolution of the system for time periods longer than the characteristic decay time one needs to provide some source of energy to the system or to introduce an external force  $f$ . Similar to the case with the Coriolis force,  $f$  in (3) corresponds to the curl part of the force.

The results of simulations of the system (3) over the time period  $t = 10^3$  with a prescribed force  $f = 10^{-2}(1 + i)$  at  $k_0 = 1$  without rotation are presented in Fig. 3. Starting from an arbitrary initial velocity field, the system (3) comes

to the statistically stable state with Kolmogorov's energy distribution, similar to the free decay case for the moment where the energy is comparable.

As was already mentioned above, the direct introduction of rotation setting  $C_r = 1$  in (7) is contradictive to the physics of the problem and to the original equation (1). It is easy to see that for the regime of the fast rotation ( $R_o \ll 1$ ) in the original Navier-Stokes equation (1), when  $V < R_o$ , the balance between the pressure and the potential parts of the forces  $f$  and  $F_c$  holds. Such a balance of the pressure and the Coriolis force, which takes place, e.g., in the Earth's liquid core ( $E = 10^{-15}$ ,  $R_o = 4 \cdot 10^{-7}$ ), is called the geostrophic balance (in the present dimensionless units regime the Earth's core situation corresponds to  $R_o V < 10^{-3}$ ). Exclusion of the pressure requires exclusion of the potential parts of all the forces, too. Then, the remaining curl parts of the forces are already of the same order as the inertial term and it is these parts which are in the r. h. s. of (3). These considerations can be formulated as follows:

$$\begin{cases} C_{rn} = R_o k_n |u_n|, & R_o k_n |u_n|^2 < |u_n| \\ C_{rn} = 1, & R_o k_n |u_n|^2 > |u_n|. \end{cases} \quad (11)$$

In other words, condition (11) means that for all wave numbers where the Coriolis force is larger then the non-linear term it must be compensated by the pressure, and its curl part ( $F_c$ ) must be of the same order as the non-linear term. (An example of violation of the condition (11) will be also considered below.) The suggestion (11) is also supported by the recent paper [12], where the scaling law  $\sim k^{-2}$  for the geostrophical balance was derived.

The results of simulations with rotation and  $C_r$  defined by (11) are presented in Fig. 3. As in the free decay case we observe two regimes with slopes  $\sim k^{-2}$  for the small wave numbers and the Kolmogorov's regime  $\sim k^{-5/3}$  for the wave numbers  $k > k_\Omega$ . It is easy to see that in this model the non-linear term has a white spectrum for  $k < k_\Omega$ . Due to the condition (11), the curl part of Coriolis term  $F_c$  has the same distribution in the wave space. This state of equipartition was observed after averaging. Analysis of the phases of the non-linear term and the Coriolis term reveals the existence of anticorrelation. This is the reason why the spectrum of the rotating turbulence decreases faster then Kolmogorov's one. In fact, the Coriolis force partially locks the energy transfer from large to small scales. Moreover, the Coriolis force blocks the applied external force, so that  $F_{c0} = -f_{c0}$  and suppresses injection of the energy into the system (3, 7, 11).

To demonstrate this phenomenon we present calculations with  $C_r$  ten times larger then was predicted by (11) (dotted line in Fig. 3). This regime shows very strong blocking. Our calculations show that the further increase of the Coriolis term leads to a degeneration of the spectrum at all. The solution then

has a singular spectrum and the whole energy is concentrated at the wave number  $k_0$  where the force  $f$  is applied.

We also present results of calculations with a prescribed force of the form  $f_0 = 0.1(1 + i)/u_0^*$  which allows us to define the exact amount of energy injected into the system. It appears that the introduction of rotation leads to an increase of the total energy of the system due to a decrease of the energy dissipation in the cascade, see Fig. 4. Note that the similar effect in 3D numerical simulations [7], where the external force was applied at some intermediate scale, was caused by the inverse cascade.

## 6 Helicity generation

As follows from (5) in 3D case ( $\epsilon = 1/2$ ) the explicit form for helicity is

$$H = \sum_n (-1)^n k_n |u_n|^2. \quad (12)$$

However, the direct application of formula (12) for the estimation of helicity or the calculation of  $\alpha$ -effect can lead to misleading results. Additional assumptions on the physics of the process are required. To understand the nature of the problem we will recall some basics of the mean-field dynamo theory, where the models of helicity for the rotating bodies were extensively studied.

According to [13], the mean helicity in the rotating body is defined as  $\mathbf{H} = \langle \mathbf{V} \cdot (\nabla \times \mathbf{V}) \rangle$ , provided that the gradient of the density exists ( $\langle \dots \rangle$  means mean average). This problem reflects the statistical inequality of the left-side and right-side rotating curls. In its turn, such inequality is caused by existence of the selected direction ( $\mathbf{z}$ ), which is related to the global rotation of the considered body. In absence of rotation the generated helicity has stochastic temporal behavior and zero mean level. Moreover, in the case of the Kolmogorov's turbulence with  $E(k) \sim k^{-5/3}$ , the helicity  $H$  has an increasing spectrum  $\sim k^{1/3}$  and its amplitude will be defined by the velocity field near the Kolmogorov's cut-off wave number  $k_d$ <sup>1</sup>. The temporal behaviour of the helicity for the case of the non-rotating homogeneous turbulence (with all other parameters are equal to the case with forcing in section 5 and summation in (12) is over the whole range of wave numbers) is presented in Fig. 5a. We observe high frequency oscillations with the negligible mean level ( $\overline{H} \sim 10^2$ ).

<sup>1</sup> Note that for the dynamo applications the maximal wave number in the sum (12) is limited by the condition  $r_m \geq 1$ , where  $r_m$  is the micro-scale magnetic Reynolds number.

This case can hardly describe the helicity observed in astrophysical and geophysical bodies with a stable sign over time periods much longer than the characteristic convective times [14].

Application of the Coriolis force in the form (7) does not change the situation essentially. In Fig. 5b we present calculations of  $H$  for the previously considered regime with rotation (Fig. 1). Even now, when the helicity spectrum is white ( $\sim k^0$ ) and correspondingly contributions of the high harmonics are smaller than in the Kolmogorov's turbulence, the helicity behavior exhibits strong oscillations with asymptotically zero mean level ( $\overline{H} \sim 10^1$ ).

To estimate which part of helicity is produced in the rotational part of the spectrum ( $k < k_\Omega$ ) we limit the cut-off wave number in (12) to  $k_{MAX} = k_\Omega$ , see Fig. 5c. This filtering decreases the dispersion of the helicity, but still does not change its mean level ( $\overline{H} \sim 10^1$ ).

To overcome the problem of zero mean level of helicity we have to introduce an additional asymmetry in the system (3,7). So far in our homogeneous incompressible shell model the gradient of the density is absent, so we have to include the missing effect in the Coriolis force:

$$F_c = -iC_r u(1 + C_1(-1)^n), \quad (13)$$

where  $C_1$  is a real constant. The results of simulations with  $C_1 = 4$ ,  $k_{MAX} = k_\Omega$  are presented in Fig. 5d. In this case  $\overline{H} \sim 140$  and is comparable with the amplitude of the oscillations. The corresponding spectrum for this regime has the same behavior as in the case when the Coriolis force was defined by (7), see Fig. 3.

## 7 Conclusions

The proposed shell model approach description to the rotating hydrodynamical turbulence demonstrates the principal possibility to reproduce the scaling law  $\sim k^{-2}$  predicted in [4], [5]. This deviation from the homogeneous Kolmogorov's turbulence represents the reduction of the 3D space problem toward 2D space, where the direct cascade of enstrophy already has  $\sim k^{-3}$  slope. In terms of the shell models one can solve the Cauchy problem for evaluating rotating turbulence and mimic its dynamical behavior in time. As was mentioned, the problem of rotating turbulence has applications to the liquid core of the Earth. The estimate of the Reynolds number based on the west drift velocity and molecular viscosity gives  $Re \sim 10^9$ , which is out of reach of any modern supercomputers in 3D direct numerical simulations. The situation in many other astrophysical bodies is even more dramatic where the estimates



of the Reynolds number give  $Re \gg 10^{10}$  [14]. This Reynolds number is no problem in the shell model, where the wide range of scales can be covered by a few harmonics. That is why the proposed application of the shell model to the fast rotation regime is a very promising step in its development. We also realize that the mechanism of helicity generation proposed by [13] is not the only one and some forms of helicity generation different from (13) are possible. The present approach was dictated by its popularity in the mean-field dynamo model of the  $\alpha$ -effect. We plan to use the shell model developed for the computation of the subgrid processes in the 3D large-scale thermal convection problem similar to [15].

### **Acknowledgements**

RM is grateful to Central Institute for Applied Mathematics (ZAM) of Forschungszentrum in Jülich for hospitality. This work was supported by the Russian Foundation of Basic Research (grant 03-05-64074). RM express his gratitude to Peter Frick for discussions.

## References

- [1] P. Tabeling, Phys. Reports. 362 (2002) 1.
- [2] U. Frisch, Turbulence: the Legacy of A.N. Kolmogorov, Cambridge University Press, Cambridge, 1995.
- [3] G. K. Batchelor, The Theory of Homogeneous Turbulence. Cambridge University Press, Cambridge, 1953.
- [4] O. Zeman, Phys. Fluids. 6 10 (1994) 3221.
- [5] Y. Zhou, Phys. Fluids. 7 8 (1995) 2092.
- [6] R. H. Kraichnan, Phys. Fluids. 8 (1965) 1385.
- [7] M. Hossain, Phys. Fluids. 6 4 (1994) 1077.
- [8] L. Jacquin, O. Leuchter, C. Cambon, J. Mathieu, J. Fluid Mech. 220 (1978) 1.
- [9] T. Bohr, M. Jensen, G. Paladin, A. Vulpiani, Dynamical Systems Approach to Turbulence, Cambridge University Press, Cambridge. 1998.
- [10] C. A. Jones, Phil. Trans. R. Soc. London, A 358 (2000) 873.
- [11] P. Frick, B. Dubrulle, A. Babiano, Phys. Rev. E, 51 6 (2002) 5582.
- [12] P. Constantin, Phys. Rev. Lett. 89 18 (2002) 184501.
- [13] F. Krause, K.-H. Rädler, Mean Field Magnetohydrodynamics and dynamo theory, Akademie-Verlag, Berlin. 1980.
- [14] Ya. B. Zeldovich, A. A. Ruzmaikin, D. D. Sokoloff, Magnetic fields in astrophysics, NY. Gordon and Breach, 1983.
- [15] P. Frick, M. Reshetnyak, D. Sokoloff, Europhys. Lett. 59 (2002) 212.

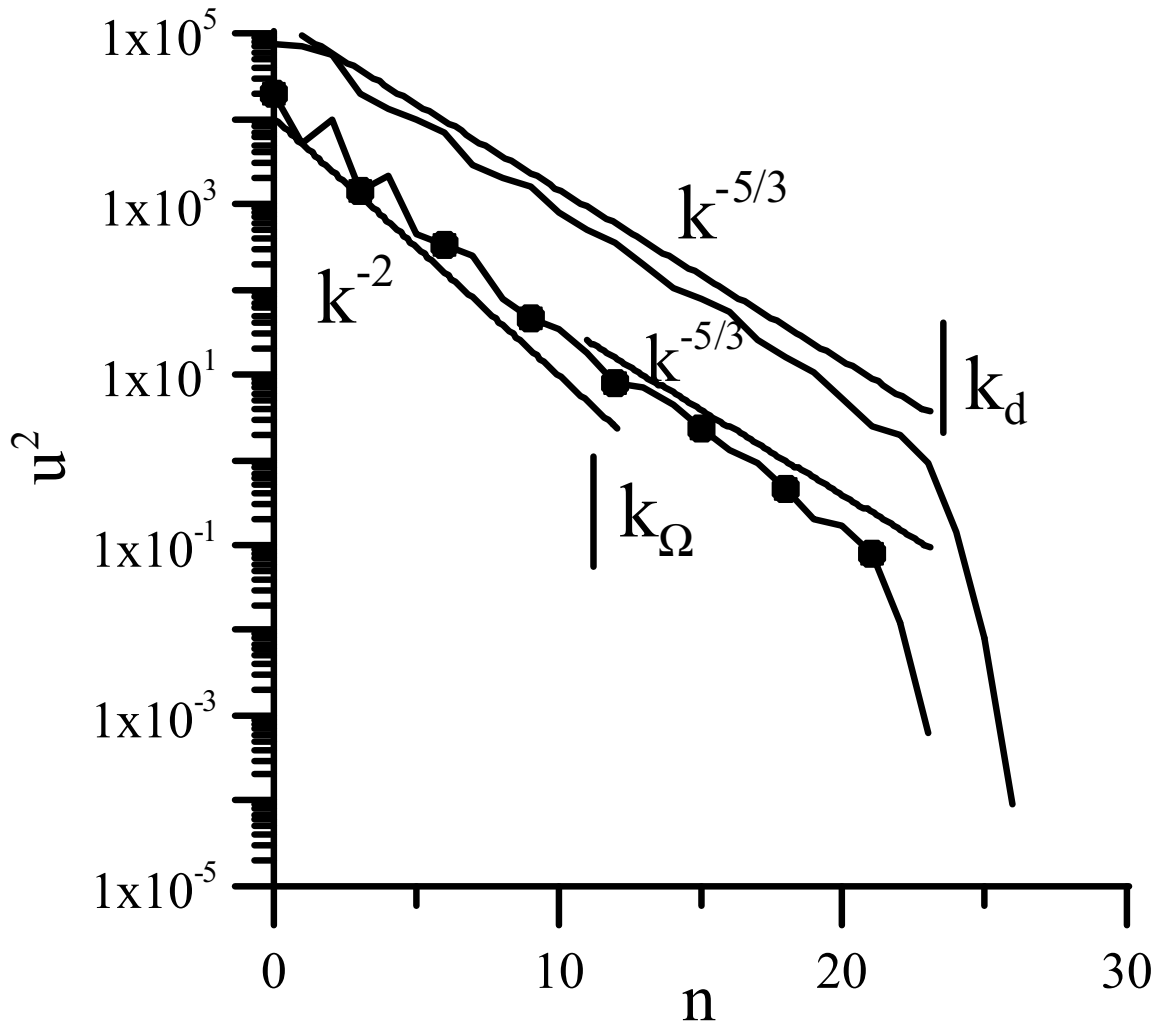


Fig. 1. Spectra of the free decay hydrodynamical turbulence,  $E = 10^{-10}$ ,  $R_o = 10^{-3}$ . Solid line corresponds to the regime without rotation,  $C_r = 0$ , and line with circles to the regime with rotation,  $C_r = 1$ .

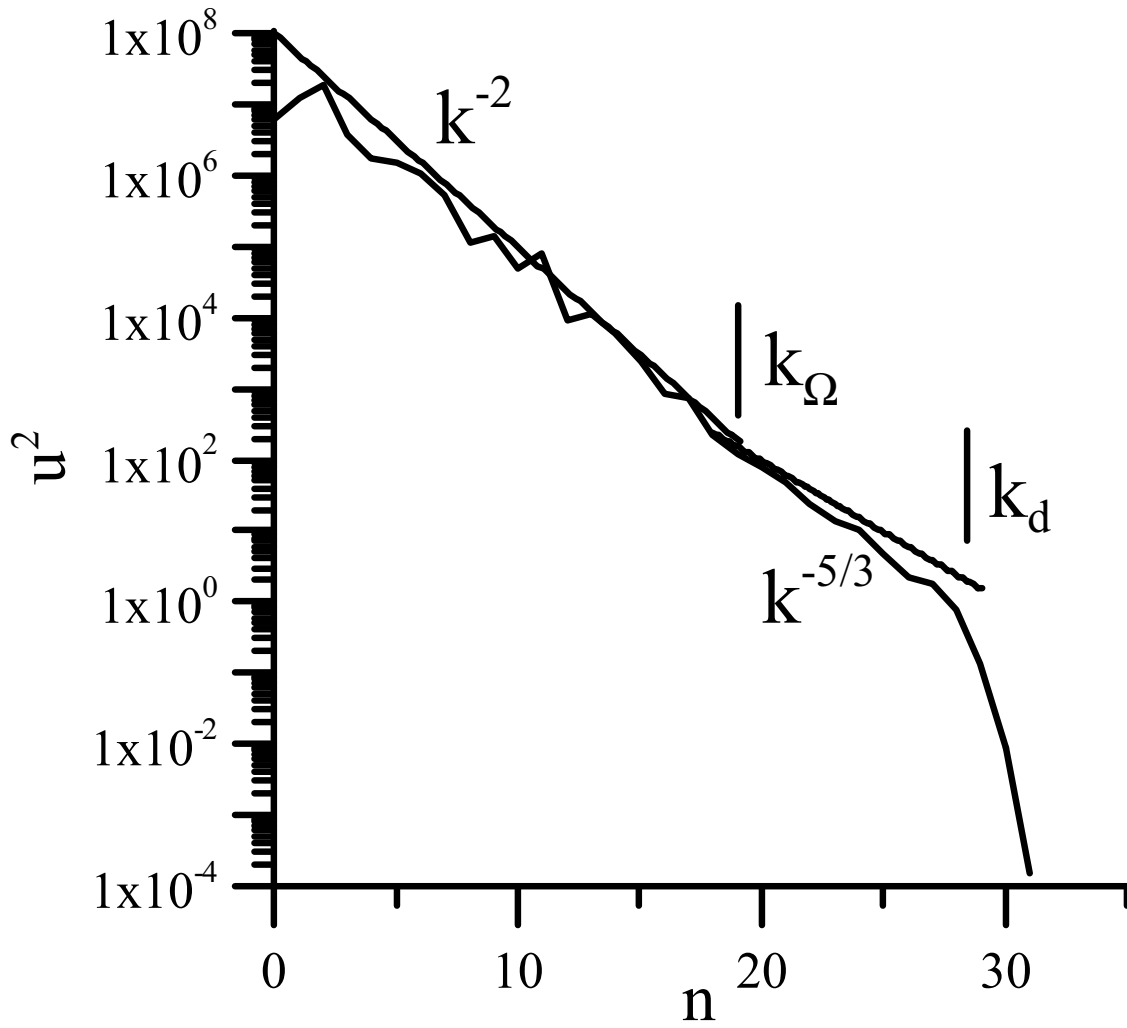


Fig. 2. Spectra of the free decay rotating turbulence,  $E = 10^{-15}$ ,  $R_o = 4 \cdot 10^{-7}$ ,  $C_r = 1$ .

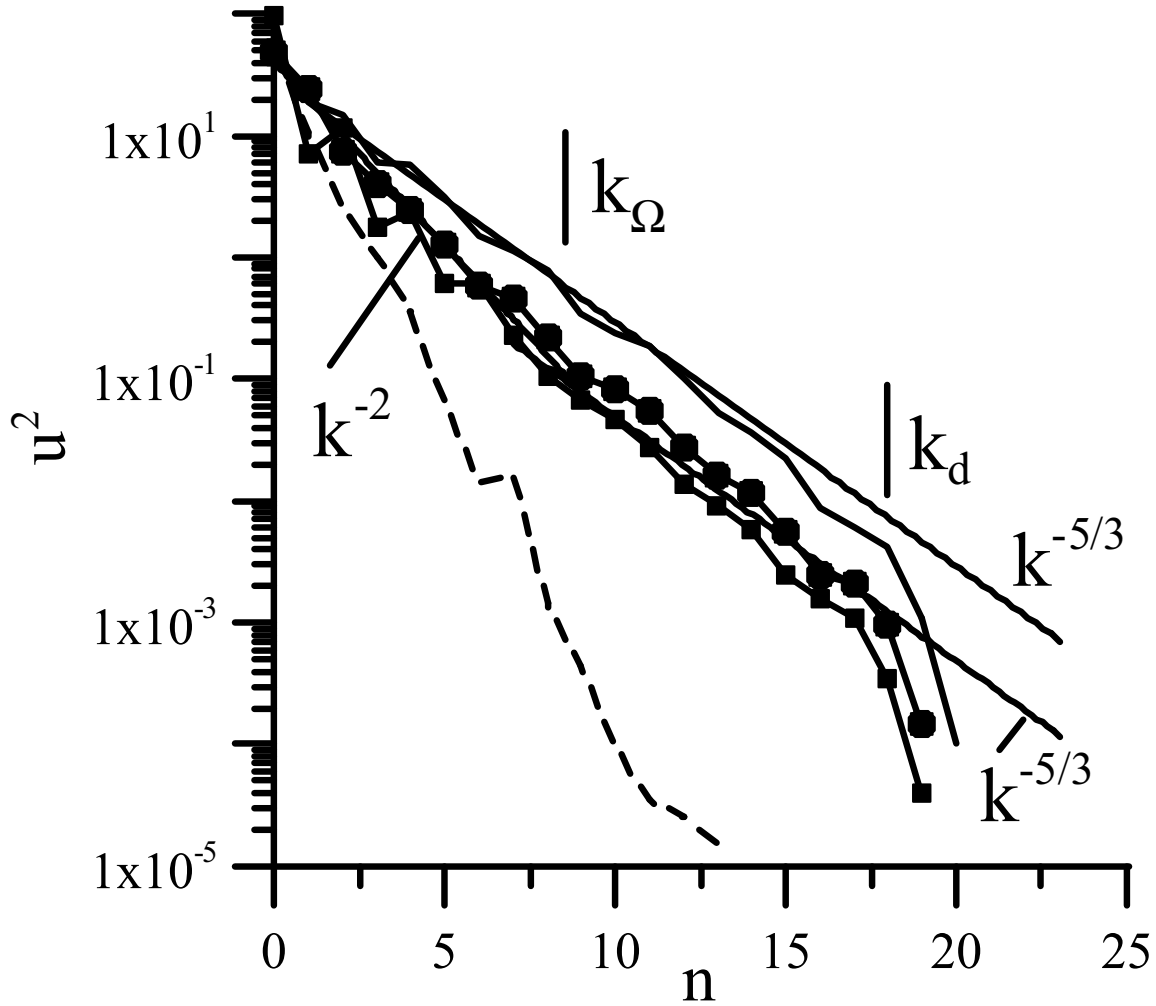


Fig. 3. Spectra of the turbulence with external forcing  $f_0 = 10^{-2}(1 + i)$ ,  $E = 10^{-10}$ ,  $R_o = 10^{-3}$ . Solid line corresponds to the regime without rotation,  $C_r = 0$ ; line with circles corresponds to the regime with rotation,  $C_r = 1$  and the Coriolis force defined by (7); the dotted line to  $C_r = 10$ . The line with squares corresponds to the modified Coriolis force (13).

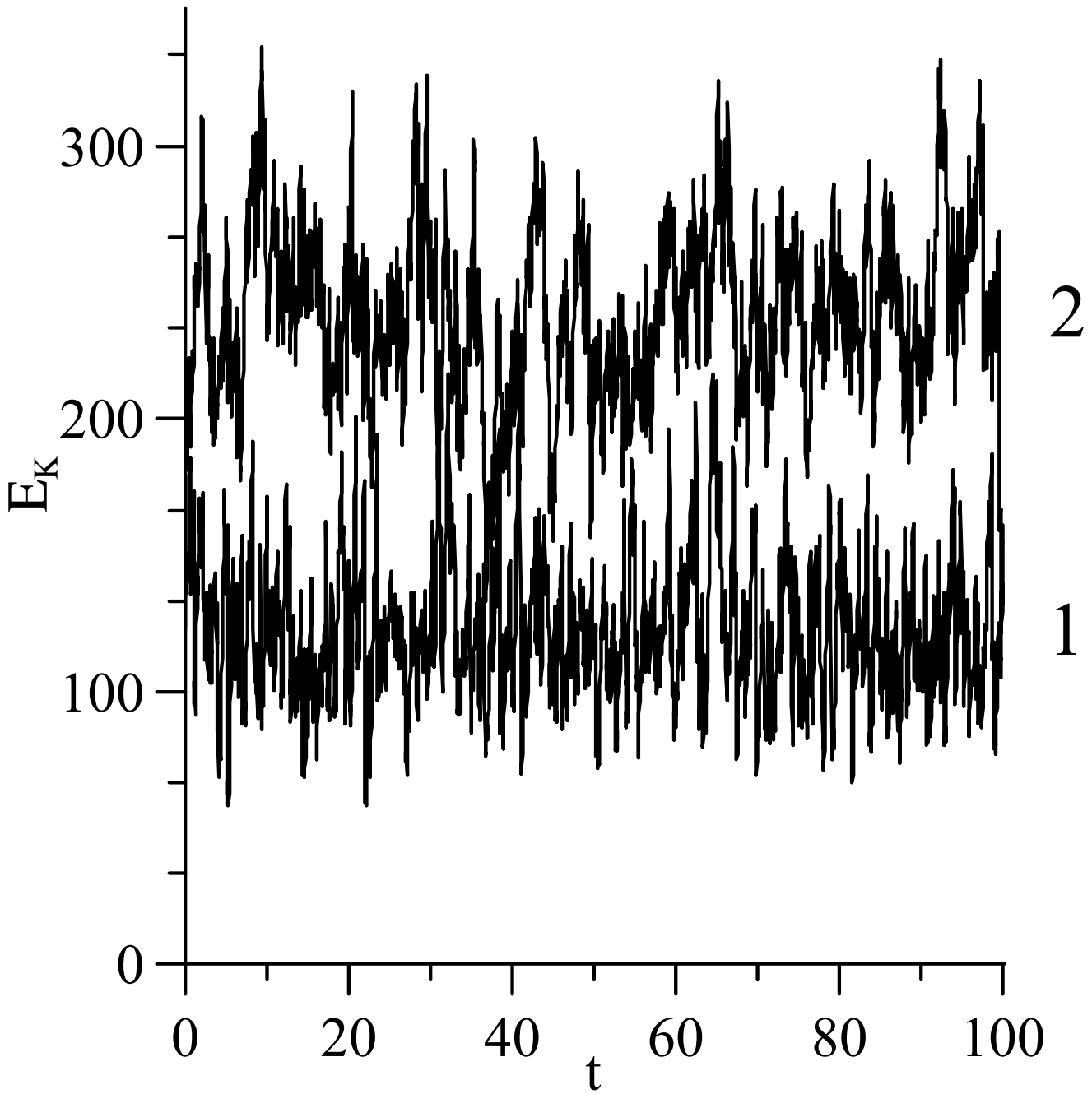


Fig. 4. Evolution of the kinetic energy  $E_k$  for the non-rotating (1) and rotating (2) turbulence,  $f_0 = 10^{-1}(1 + i)/u_0^*$ ,  $E = 10^{-10}$ ,  $R_o = 10^{-3}$ .

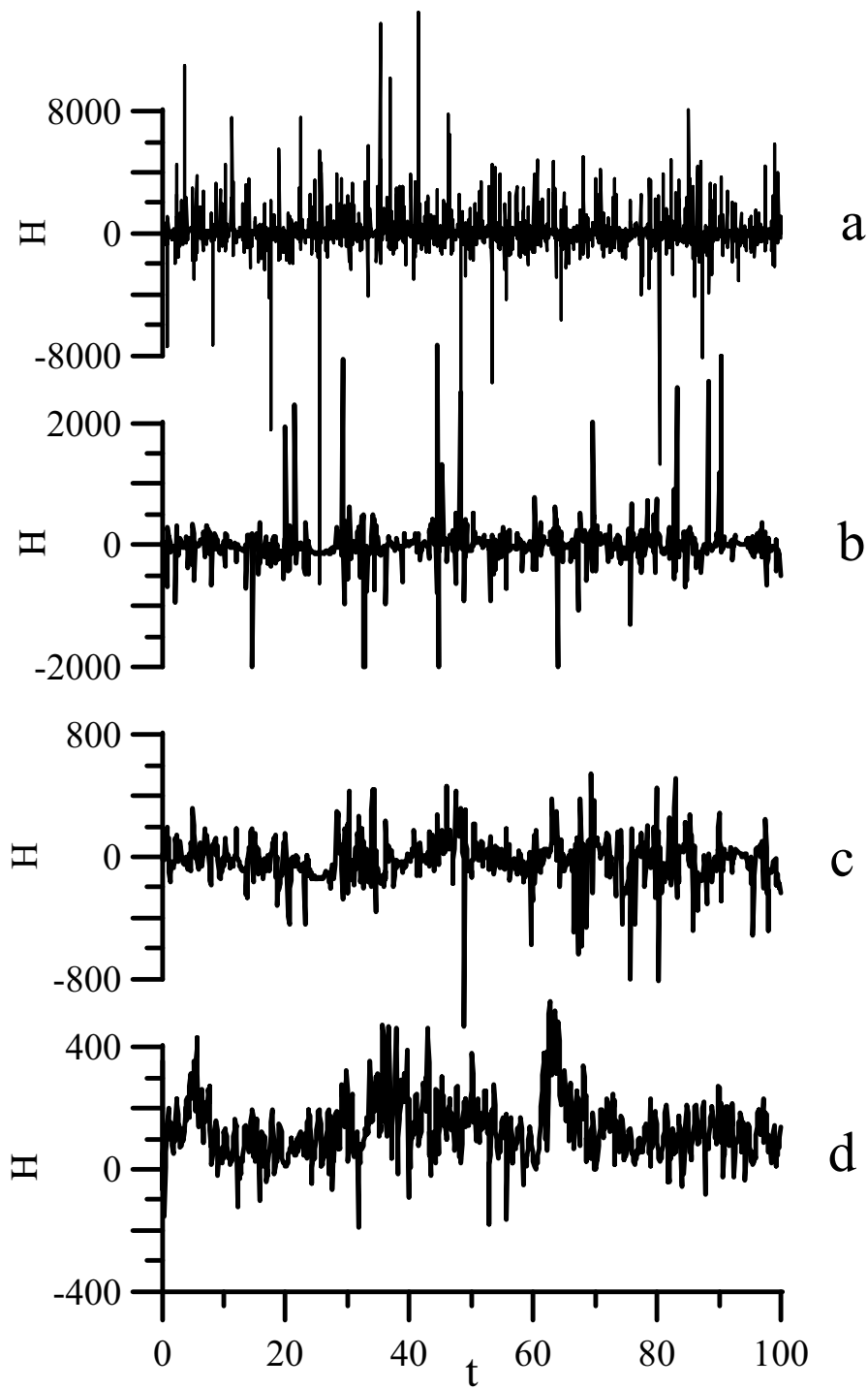


Fig. 5. Time evolution of helicity  $H$ . The curve (a) corresponds to the non-rotating (Kolmogorov's) turbulence; curve (b) is the regime with the Coriolis force defined by (7); case (c) is the same to (b) but with cut-off at  $k_\Omega$  (only  $k \leq k_\Omega$  in (12)) and case (d) with the Coriolis force defined by (13) and  $k \leq k_\Omega$ .